Available online at www.sciencedirect.com
SCIENCE DIRECT®
Journal of Sound and Vibration 274 (2004) 669–683
JOURNAL OF SOUND AND VIBRATION
www.elsevier.com/locate/jsvi

Assessment of the diffraction efficiency of novel barrier profiles using an MLS-based approach

G.R. Watts, P.A. Morgan*, M. Surgand

Environment Group, TRL Limited, Old Wokingham Road, Crowthorne, Berkshire RG45 6AU, UK

Received 29 January 2003; accepted 29 May 2003

Abstract

In recent years there has been growing interest in the use of noise barrier profiles that can enhance the diffraction efficiency of plane barriers. These are placed on the top of the barrier in order to reduce sound diffracted into the shadow zone. A variety of shapes have been tested including T-shapes, multiple-edges and various cylindrical configurations. Despite numerous demonstrations that the profiles enhance performance there is no universal agreement on how the improvements can be quantified and incorporated into noise prediction models. Without such quantification it is likely that such profiles will not receive widespread acceptance. TRL has carried out an experimental investigation of the performance of novel-shaped barriers for the Transport Research Foundation. The approach relies on quantifying diffraction efficiency in the near field using a novel application of the Maximum Length Sequence (MLS)-based method. Measurements on 4 different profiles were taken in the vertical plane perpendicular to the barrier face. Two source and four receiver positions were used and results were obtained under a range of wind conditions. Results show large differences between the efficiency of the different options with the absorptive T-shaped and multiple-edge profiles performing best.

1. Introduction

Noise barriers are frequently employed in highway design to help mitigate the impact of traffic on roadside communities. The screening performance of barriers is dominated by sound that is diffracted over the top. In recent years there has been considerable interest in designing barrier profiles that are more efficient at improving screening performance over that provided by a simple thin screen. To widen and encourage the use of these innovative barrier profiles there is a need to be able to simply characterize their acoustic performance.

*Corresponding author. Fax: 44-1344-770918.
E-mail address: pmorgan@trl.co.uk (P.A. Morgan).

0022-460X/$ - see front matter © 2003 TRL Ltd. Published by Elsevier Ltd. All rights reserved.
doi:10.1016/j.jsv.2003.05.005

The European Standards Group CEN TC 226/WG6 has developed draft standards on measuring in situ absorption and transmission loss of noise barriers [1]. There is currently interest from European highway authorities in developing a method to quantify the diffraction efficiency of devices which can be added to the top of a noise barrier. Such add-on devices can take a variety of forms including multiple-edge profiles, absorptive T-shapes and rounded caps. This paper[1] describes an investigation of the performance of such devices using a novel application of the Maximum Length Sequence (MLS)-based method to characterize diffraction efficiency. The main advantage of this approach is that measurements can be taken in situ in the presence of high extraneous noise, e.g., at the edge of a busy motorway. For the purpose of this study, however, the measurements were carried out at TRL's experimental noise barrier facility.

From a practical point of view, it is the performance in the far field that is generally of greater importance. In any extension of the work described in this paper, the results of measurements made close to the barrier should be compared with results at greater distances. This would allow the most appropriate measurement set-up for MLS-based measurements to be determined.

2. Theory

Time domain analysis techniques can, in theory, be used to determine the diffraction efficiency of a roadside noise barrier. Essentially, the method requires the generation of a known acoustic signal using a loudspeaker located on one side of the barrier and a receiver microphone located in the shadow zone behind the barrier. Using suitable windowing of the receiver signal, the component of the generated signal that is diffracted over the barrier, i.e., the diffracted impulse response, can be determined. In a similar way the attenuation due to free-field propagation can be determined using the same set-up but without the barrier and the ratio between the diffracted and free-field impulse responses then offers a measure of the attenuation provided by the barrier. Provided the generated signal can be uniquely identified, the measurements can be taken in the presence of other extraneous noise such as traffic noise. In theory, therefore, the technique should be applicable to determining barrier efficiency in situ.

To investigate the diffraction efficiency of noise barrier profiles, the experimental set-up shown in Fig. 1 was used. In the diagram, it can be seen that the microphone is located in the shadow zone so ensuring that the diffracted component of the impulse response will be considerably greater than any transmitted components. In this study the sound generation, measurement and preliminary analysis were performed using a commercial package, MLSSA, which is based upon research carried out by Rife and Vanderkooy [2]. This package provides the hardware and software needed to generate the required signal at the loudspeaker and the time windowing and Fourier transform software used in the analysis. It should be noted that in addition to the basic MLSSA package all other acoustic analysis procedures were developed by TRL using the software platform MATLAB.

[1] The research reported in this paper was commissioned as part of the Transport Research Foundation's ongoing programme of scientific research. All rights to the intellectual property within the document remain with the Transport Research Foundation.

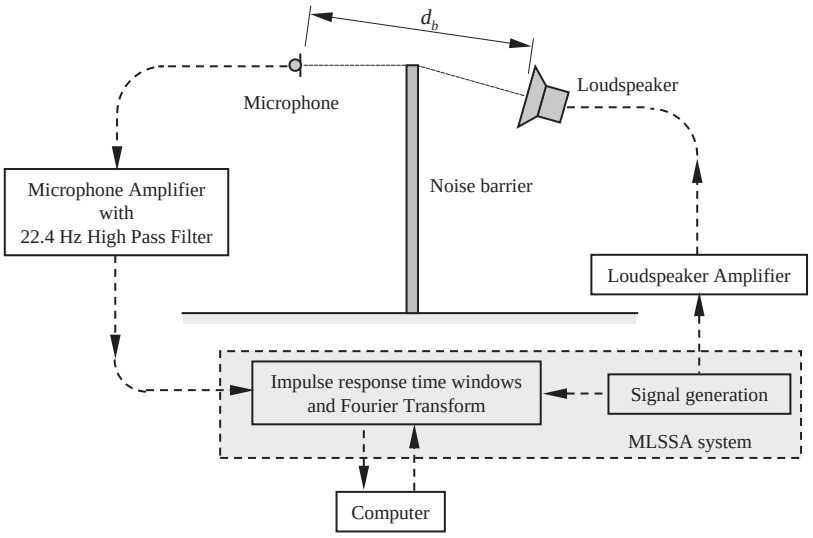

Fig. 1. Measurement set-up for characterizing the diffraction efficiency of a noise barrier.

The insertion loss (the level difference with and without the barrier present) is given by

$$\mathrm{IL}(f) = -10 \times \log\left\{\frac{|H_b(f)|}{|H_i(f)|} \times \frac{d_b}{d_i}\right\}^2 \mathrm{dB}, \tag{1}$$

where $H_b(f)$ is the frequency response of the diffracted component impulse response, $H_i(f)$ is the frequency response of the free-field impulse response, and d_b and d_i are the lengths of the shortest direct path through the barrier and the path length used for the free-field measurements, respectively.

3. Experimental investigation

In order to examine the performance of the method, measurements were carried out at full scale on a range of barrier profiles using TRL's purpose-built experimental barrier facility.

3.1. Barrier profiles investigated

The cross-sectional designs of the different barriers tested, together with appropriate dimensions, are shown in Figs. 2 and 3. For each barrier the main upright was 2.0 m high, 5.0 m long, 0.12 m thick and formed from 2 bays. Each bay was comprised of a 0.5 m high plane concrete plinth at the base and three aluminium box-section panels (dimensions $2.5 \times 0.5 \times 0.12$ m) held in place between vertical I-section steel beams (as shown in Fig. 2). All these surfaces were acoustically reflective. The sound insulation value of the barrier was high, being over 40 dB at 1000 Hz.

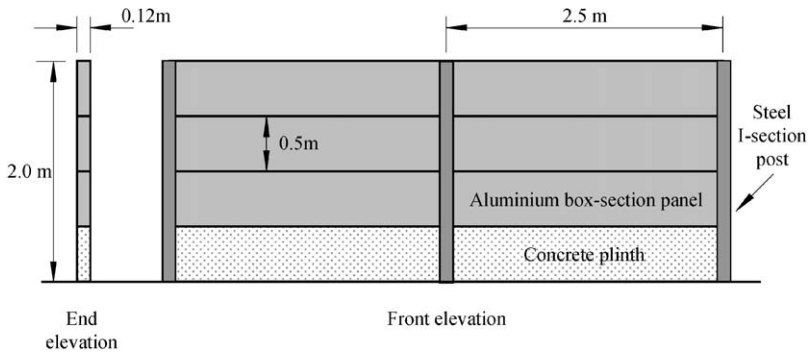

Fig. 2. Configuration of plane barrier profile tested on the Noise Barrier Test Facility.

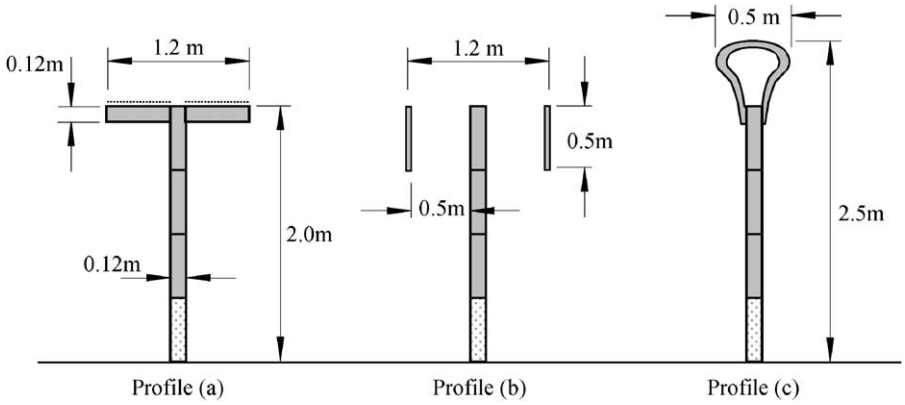

Fig. 3. Barrier profiles tested during study: (a) T-shaped barrier (dotted line denotes absorptive surface for the absorptive T-shape tests); (b) multiple-edge profile; (c) plane barrier with rounded hollow cap.

For the T-shaped barrier, shown in Fig 3(a), the crosspiece was formed from two of the aluminium box-section panels, positioned perpendicularly to the upright using a lightweight aluminium support frame attached to the main posts, such that the overall height of the plane barrier was not increased. The panels used featured a sound absorptive face on one side and a reflective face on the other. The absorptive face was formed from a perforated facing and a rockwool material. This resulted in this side of the panel having a mean absorption coefficient of $\alpha > 0.8$ (over the frequency range 0.25–5.0 kHz). The other side of the panel was constructed from un-perforated aluminium sheet and was therefore highly reflective. To create the absorptive T-shape profile shown in Fig. 3, the absorptive face was placed uppermost, whilst to create a reflective T-shape, the panels were turned so that the reflective face was uppermost.

The multiple-edge barrier, shown in Fig. 3(b), consisted of two additional side panels, attached parallel to the main upright, one on either side (separation = 0.5 m), using light structural steel beams attached to the main posts to produce a design symmetrical about the vertical axis. The panels, constructed from thin sheet steel, were 0.5 m high and positioned with the upper edge flush with the top of the main barrier. The original concept of this design i.e., multiple diffracting edges

on a single foundation, was jointly invented by TRL and the University of Bradford [3,4]. Patents were successfully applied for and the design tested.

The rounded cap fitted to the plane barrier, as shown in Fig. 3(c), was a commercial product, and consisted of a curved hollow profile. The outer surface of the profile was a perforated polycarbonate sheet that enveloped a 50 mm thick layer of mineral wool protected by a water- and UV-proof film. The absorption properties of the cap were not specified.

The overall set-up was therefore novel in that the performance of new designs of barrier profile could be investigated at full scale, outside and in the presence of non-homogeneous atmospheres. In this way the experimental conditions were capable of representing the roadside situation.

3.2. Measurement method

A loudspeaker source and microphone were placed on opposite sides of the barrier under test and set at different heights for different inclinations in the vertical plane. The loudspeaker used was a 20 W speaker having a diaphragm of 150 mm diameter and with the tweeter disabled so as to obtain a single source of sound. The microphone was a $\frac{1}{2}$ in condenser microphone. All measurements were performed with the loudspeaker and receiver microphone axis perpendicular to the top edge of the barrier, i.e., normal incidence in the horizontal plane.

Two source positions and four microphone positions were used for each barrier configuration, resulting in 8 measurement combinations per configuration. For all of the barrier configurations, the same source/receiver heights were applied relative to the leading/trailing diffracting edges of the barriers, resulting in constant angles of inclination. The horizontal separation between the barrier and these source/receiver positions was set at 1.0 m from the position of the leading/trailing diffracting edges, respectively. These positions are summarised in Table 1 and illustrated in Fig. 4 relative to the multiple-edge barrier.

For the barrier with the rounded cap, the position of the diffracting edge was defined as the tangent point for the line of sight from any source or receiver position. Consequently, the lower sources and receivers were further from the barrier centre than for any of the other options.

The orientation of the selected sources corresponded to the angles which would be defined by a 3 m high barrier were the sources to be located in the middle of the nearside and farside carriageways of a typical motorway (S_1 and S_0, respectively). The orientation of the receiver positions corresponded to the angles which would be defined by a standing adult at distances of

Table 1
Source and receiver heights used for measurements on Noise Barrier Test Facility

Source identifier	Vertical position below top of barrier (m)	Inclination θ_s (deg)	Receiver identifier	Vertical position below top of barrier (m)	Inclination θ_r (deg)
S_0	0.11	6.3	M_1	0.00	0.0
S_1	0.36	19.8	M_2	0.05	2.9
			M_3	0.15	8.5
			M_4	0.30	16.7

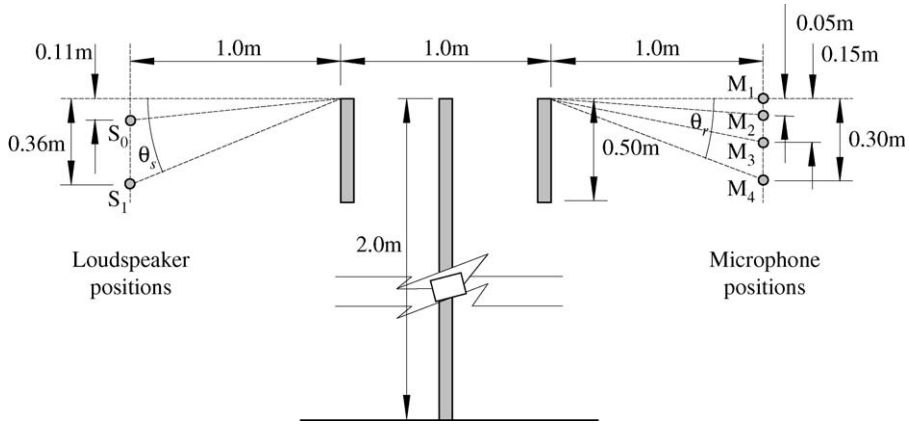

Fig. 4. Positions of source and microphone relative to multiple-edge barrier profile.

30, 10 and 5 m from the 3 m high barrier (M_2, M_3 and M_4, respectively). The receiver level with the barrier top (M_1) would of course be at a large distance from the barrier.

For each individual measurement combination, the MLSSA analysis software was configured to use 16 averages and an MLS order of 15 (i.e., a sequence length of 32,767 samples or 0.74 ms). To reduce the disruptive influence of wind on the measurements, it was necessary to introduce a filter into the measurement set-up to filter out frequencies below 22.4 Hz.Without the filter, the measurements took longer to record because many samples were flagged as invalid by the acquisition software. This may have resulted from the high spurious low frequency components produced by the turbulent air stream around the microphone. This filter was applied at the microphone amplifier (as shown in Fig. 1).

It was known that wind can have a deleterious effect on the performance of a noise barrier in the far field due to turbulent scattering of sound waves into the shadow zone of the barrier and by refraction caused by wind speed gradients. However, it was not known if this would affect results close to the barrier edge. To take account of this possible effect, an anemometer (wind-tracker) was used in order to keep a record of the wind speed and direction over the duration of the measurements. The component of the wind vector perpendicular to the plane of the barrier was averaged over the period of each measurement. In general, for each barrier/source/receiver geometry, 4 repeat measurements were taken with a positive wind vector and 4 measurements taken with a negative wind vector. This was achieved by carrying out a set of measurements for each geometry, swapping the positions of the loudspeaker and microphone and repeating the measurements. With a total of 8 repeat measurements and corresponding positive and negative wind components, it was possible using linear regression to obtain a good estimate of the relationship between insertion loss and wind speed. The regression relationships were then used to determine the insertion loss at zero wind speed.

Free-field measurements were taken at the beginning and end of each measurement session. The source and microphone were placed well away from the barriers and at a height of 2.0 m above ground level. Although the length d_b in Eq. (1) changes according to the cross-sectional width of the barrier profile under study, a single free-field geometry was used for the full duration of the

measurement program, the separation d_i between loudspeaker and microphone being approximately 2.5 m.

4. Results

In addition to the comparison of experimental measurement results for the different barrier options, this section also presents comparisons between the measured values of insertion loss and those calculated using a 2-D boundary element (BEM) numerical model [5]. The model uses a Burton–Miller-type formulation to overcome any non-uniqueness of solution [6]. Since the BEM takes into account the effects of the ground plane it was necessary to remove this influence from the calculations in order to obtain a fair comparison with the measurements. This was achieved by modelling a 10 m high barrier, but keeping the positions of the microphones and sources relative to the barrier profile identical to those in the test measurements.

4.1. Comparison of barrier profiles using MLS

The insertion losses normalized to zero wind speed were plotted against frequency for each option tested. Figs. 5a and b show the results for 2 measurement positions (the microphone level with the top of the barrier and source positions 0.11 and 0.36 m below the top). The results indicate the main tendencies shown in the full set of results that have been analysed for all 8 measurement geometries, i.e., 2 source positions and 4 microphone positions.

Generally for all options there is a rise of insertion loss with increasing frequency. At the lowest frequency the insertion losses are comparable, but diverge as the frequency increases. At most frequencies the absorptive T-shape produces the greatest insertion loss and the cylinder and plane barrier the least. The largest differences are close to 15 dB(A). At the three lowest frequencies the multiple-edge profile produced the largest insertion loss while at 850 Hz and above the absorptive T-shape produced the largest effect. The performance of the reflective T-shape option tends to be intermediate lying between that of the multiple-edge and that of the plane and cylinder options.

In order to gain an insight into the performance of the barriers with typical traffic noise, a single number rating of diffraction efficiency was calculated based on a standard traffic noise spectrum given in EN 1793-3 [7]. This weights the insertion losses at a number of measured frequencies by corrections based on the third-octave A-weighted spectrum. Since the frequencies at which the insertion losses were measured were based on window length they were not at third octave centre frequencies and it was decided to select the insertion losses closest to each third octave band centre frequency.

If IL_i is the insertion loss at the ith frequency and L_i is the normalised A-weighted sound pressure level of traffic noise in the nearest third-octave frequency band, then the single number rating of diffraction efficiency SNRD is given by

$$\mathrm{SNRD} = -10 \log \left[\frac{\sum_i 10^{L_i/10} \cdot 10^{-\mathrm{IL}_{i/10}}}{\sum_i 10^{L_i/10}} \right], \tag{2}$$

where the summation is over 12 frequencies corresponding to most of the 1/3 octave frequency bands from 200 to 5000 Hz. It should be noted that in this study the measured frequency interval

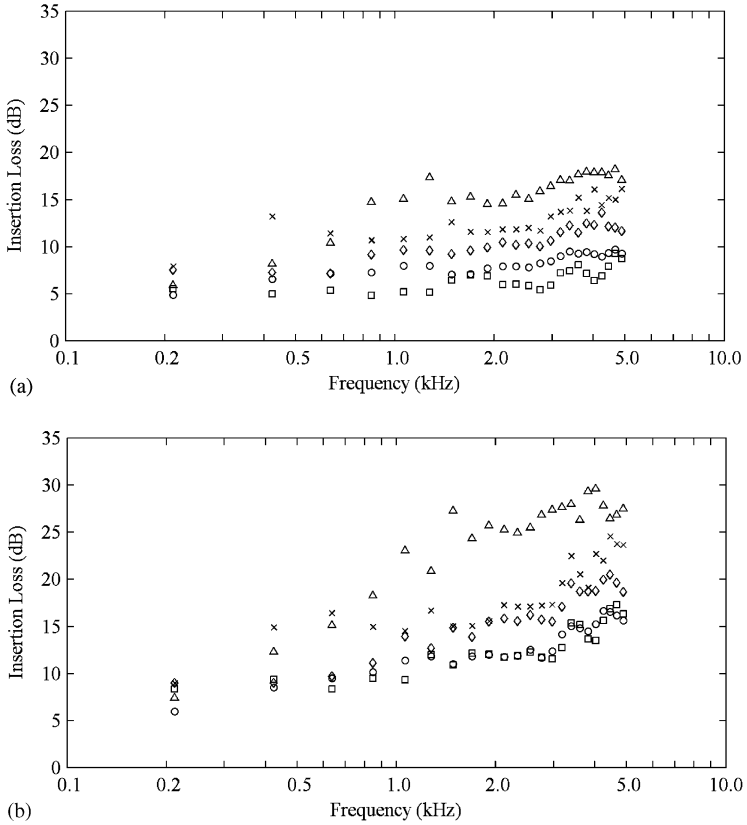

Fig. 5. Insertion loss spectra for receiver level with profile top (a) for source at 0.11 m below top of barrier and (b) for source at 0.36 m below top of barrier. (○) plane barrier, (□) rounded cap, (◇) reflective T-profile, (Δ) absorptive T-profile, (×) multiple-edge barrier.

Table 2
Single number rating by barrier option

Geometry		Single number rating of insertion loss (dB(A))				
Speaker position (m)	Microphone position (m)	Plane	Trident	Absorptive T-shape	Reflective T-shape	Rounded cap
0.11	0.00	7.5	11.3	13.2	9.2	5.6
0.11	0.05	8.3	12.1	13.9	13.3	6.7
0.11	0.15	9.6	14.0	15.2	12.1	8.5
0.11	0.30	11.5	16.3	16.4	13.8	10.6
0.36	0.00	10.9	15.3	17.8	12.4	10.4
0.36	0.05	11.5	16.2	16.1	12.9	11.2
0.36	0.15	12.6	17.8	17.0	14.8	12.9
0.36	0.30	14.2	19.9	17.3	16.0	15.5
Average:		10.8	15.4	15.9	13.1	10.2

was 212 Hz (corresponding to an effective window length of 4.7 ms). Consequently at low frequencies the spacing was too broad to include all one-third octave bands. This meant the measured levels corresponding to the 1/3 octave centre frequencies of 250, 316 and 500 Hz are missing from the above calculation. Table 2 lists the SNRDs for the 5 options tested for all the test arrangements.

It can be seen that the order of overall performance reflects the trends noted in the insertion loss spectra i.e., the absorptive T-shape and trident options showing relatively good performance but the rounded cap and plane barriers having similar relatively poor performance. The reflective T-shape shows an intermediate performance.

4.2. The influence of wind

The regression equations developed for each barrier option allowed the effects of wind to be examined at a given wind speed. However, measured wind speeds perpendicular to the barrier rarely exceeded 4 m/s so that it was not possible to examine effects at moderate to high wind speeds. As an indication of the wind effects, predictions were made at 4 m/s in the direction from source to receiver. Fig. 6 illustrates the effect of both this wind component and zero wind speed for the multiple-edge barrier, for the receiver position level with the barrier top and the source positions at 0.11 and 0.36 m below the top of the barrier. Figs. 7 and 8 plot the results for the corresponding source/receiver geometries in the presence of the reflective and absorptive T-profile barriers, respectively.

For the T-profile designs, at mid-to-high frequencies there is a noticeable wind effect generally limited to less than 5 dB. This means that noise levels will increase when the wind is blowing in the

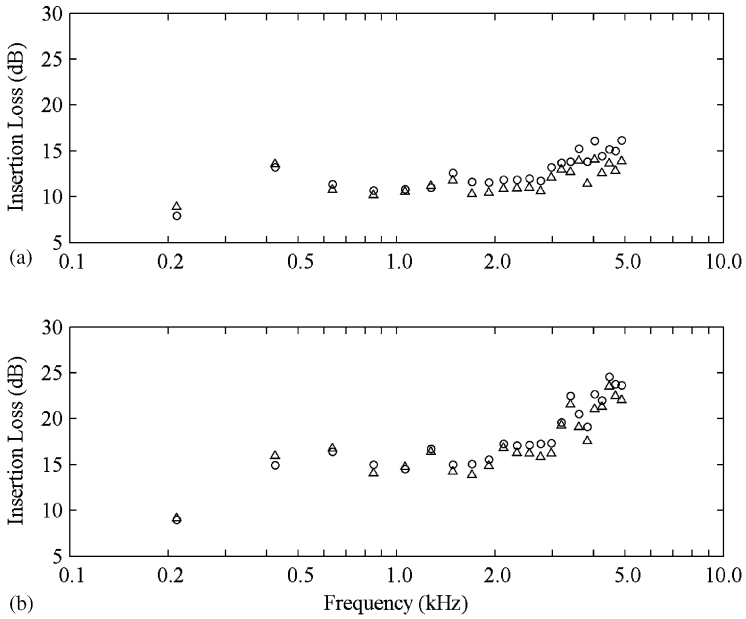

Fig. 6. Insertion loss spectra for multiple-edge barrier with receiver level with profile top (a) for source at 0.11 m below top of barrier and (b) for source at 0.36 m below top of barrier. (○) wind speed = 0 m/s, (Δ) wind speed = 4 m/s.

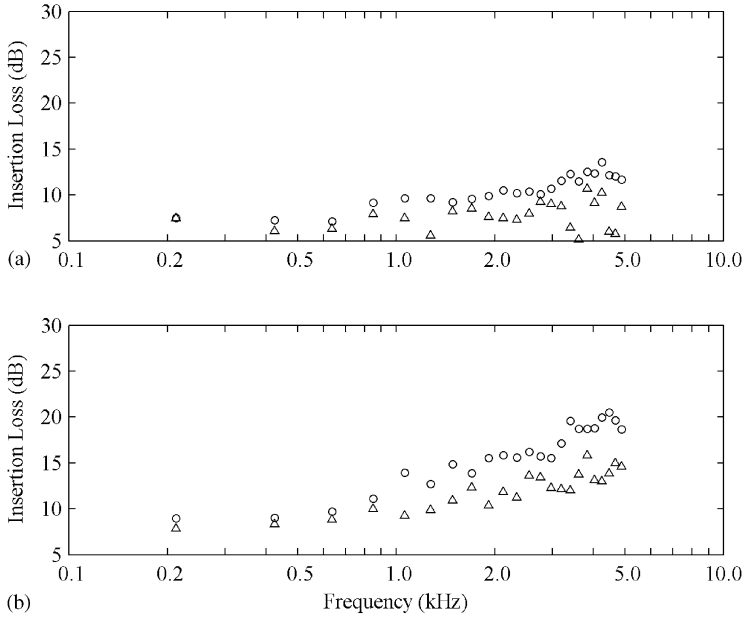

Fig. 7. Insertion loss spectra for reflective T-profile barrier with receiver level with profile top (a) for source at 0.11 m below top of barrier and (b) for source at 0.36 m below top of barrier. (○) wind speed = 0 m/s, (Δ) wind speed = 4 m/s.

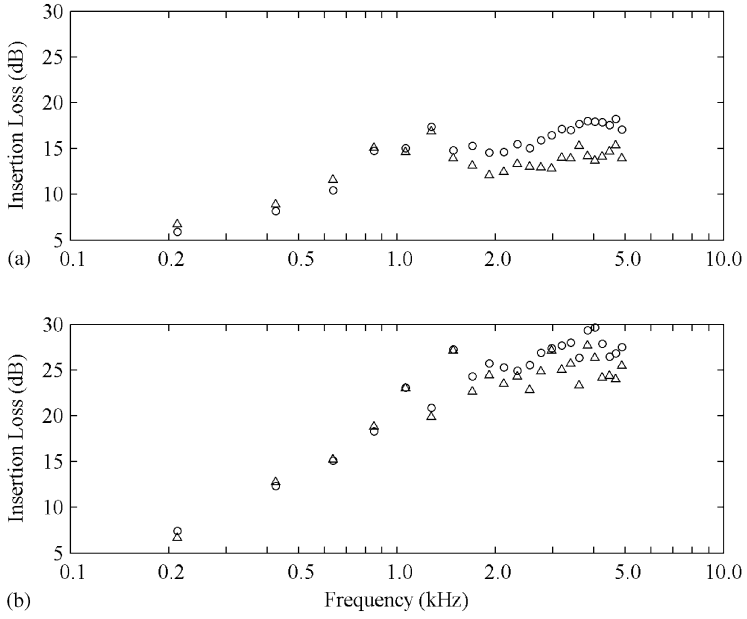

Fig. 8. Insertion loss spectra for absorptive T-profile barrier with receiver level with profile top (a) for source at 0.11 m below top of barrier and (b) for source at 0.36 m below top of barrier. (○) wind speed = 0 m/s, (Δ) wind speed = 4 m/s.

direction from source to receiver. The wind effect is considerably reduced in the case of the multiple-edge profile. It is considered that the leading diffracting edge may create turbulence that lowers the sound energy travelling over the main part of the barrier by scattering sound onto the source side of the barrier. The other two edges scatter sound into the screened area.

For the plane screen and barrier with rounded cap, the wind effects were generally of a similar magnitude to those for the multiple-edge profile.

However, because of the restricted range of winds encountered during the measurement period, it is suggested that further measurements be taken under a wider range of wind conditions in order to determine more precisely these differences in the effects of wind speed component.

4.3. Comparison with BEM results

BEM predictions were made for all of the barrier options except the barrier with the rounded cap for which values of absorption were not available. The frequencies chosen were identical to those for which measurement data was available except that at high frequencies predictions were only made for frequencies closest to 1/3 octave band centres. Fig. 9 gives the results for the multiple-edge profile with the receiver level with the barrier top and for the source in the two standard positions. The experimental data was normalised to zero wind speed since the BEM predicts for a homogeneous atmosphere. For the same source/receiver geometries, Figs. 10 and 11 plot the results for the reflective and absorptive T-profile barrier respectively. For the reflective T-profile the measured levels at most frequencies are greater than predicted. This may be due to scattering effects of the corrugations on the panels that were not included in the modelled barrier top. These corrugations were 2 cm deep and 10 cm wide.

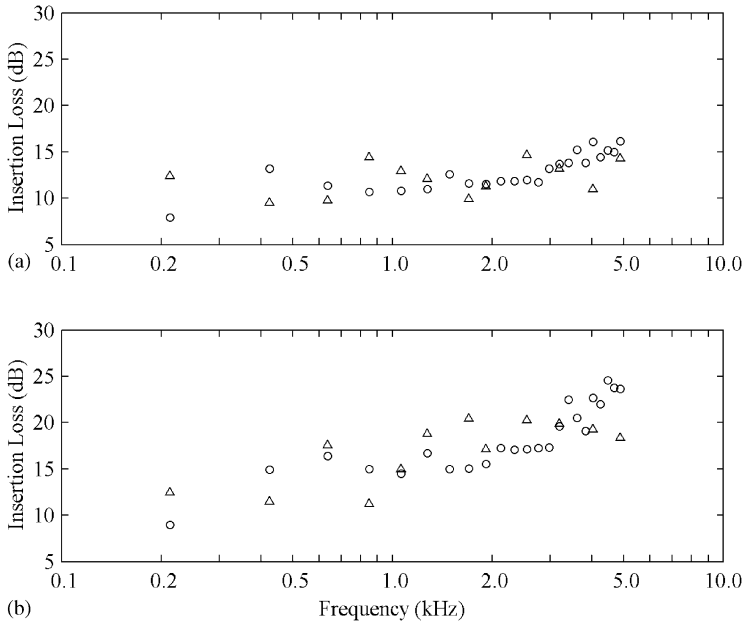

Fig. 9. Insertion loss spectra for multiple-edge barrier with receiver level with profile top (a) for source at 0.11 m below top of barrier and (b) for source at 0.36 m below top of barrier. (○) measured, (Δ) BEM prediction.

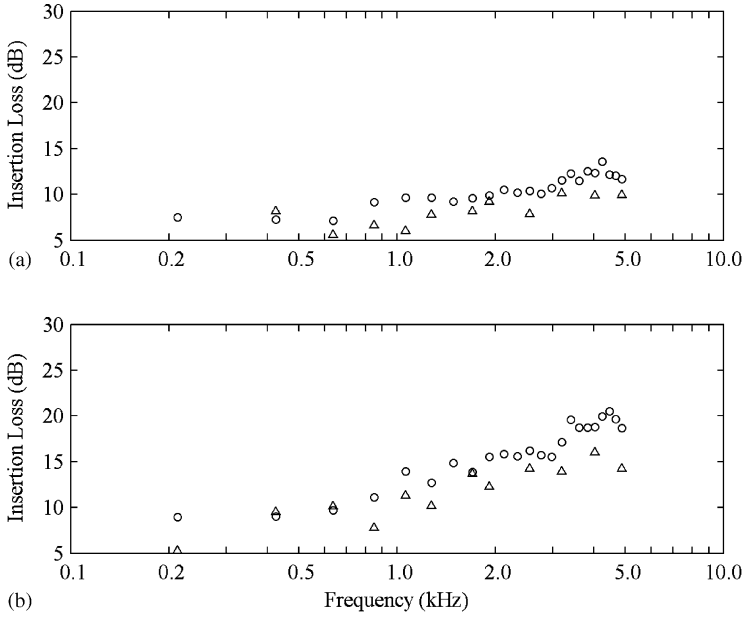

Fig. 10. Insertion loss spectra for reflective T-profile barrier with receiver level with profile top (a) for source at 0.11 m below top of barrier and (b) for source at 0.36 m below top of barrier. (○) measured, (Δ) BEM prediction.

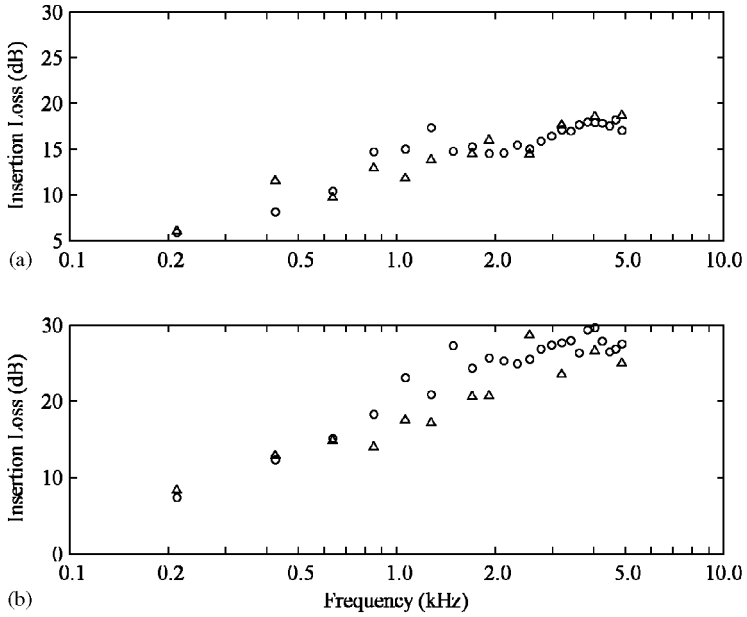

Fig. 11. Insertion loss spectra for absorptive T-profile barrier with receiver level with profile top (a) for source at 0.11 m below top of barrier and (b) for source at 0.36 m below top of barrier. (○) measured, (Δ) BEM prediction.

Generally, there is good agreement within ± 5 dB between the measured and predicted spectra, and the BEM results support the validity of the new measurement method. The MLS method provides useful experimental data for the calibration of numerical tools.

5. Discussion

The MLS-based technique using signal separation proved reliable and robust in most cases. During initial tests under windy conditions many samples were flagged as invalid by the MLSSA signal processing system. This was considered to be due to the lack of coherence between the input signal to the speaker and the output signal from the microphone that were cross-correlated during analysis to obtain the impulse response. By inserting a 22.4 Hz high pass filter in microphone amplifier this problem was significantly reduced. It is likely that the turbulence around the microphone created under windy conditions was producing high levels of low-frequency noise that may have caused distortion of the microphone signal.

It was possible to use a relatively small, low output loudspeaker (20 W) during the trials, although under high levels of ambient noise, e.g., at the roadside, it may be necessary to consider the use of a more powerful source. However, such a source should remain compact otherwise the geometry from source to diffracting edge is not well defined, since contributions can arise from the edges of the loudspeaker cone which may present a significantly different angle of incidence to that defined by the loudspeaker axis. The geometry that was developed for these tests was based upon a consideration of typical source and receiver positions in front of and behind a barrier positioned close to a typical motorway. However due to time constraints, only a single angle of incidence in the horizontal plane was used, i.e., normal incidence. Since a traffic stream can be considered as an infinite line source, to fully characterize the performance of a barrier screening traffic noise it is necessary to consider other angles of incidence. It is therefore recommended that for any future work, measurements should not be restricted to normal incidence.

The results of this study have established that this MLS-based approach is clearly sensitive enough to demonstrate differences between barrier profiles. Compared with a similar plane barrier, differences of up to approximately 15 dB were observed in the third-octave band insertion loss spectra. As expected, the use of an absorptive material on the upper surface of the T-shaped profile improved the insertion loss considerably. From Table 2, the single number rating of insertion loss for the absorptive T-shape was over 2.5 dB(A) greater than for the reflective T-shape. Similar improvements compared with the plane barrier were produced by the multiple-edge design. This works on a different principle to the absorptive T-shape profile since no absorptive material is involved. The two side panels of the multiple-edge profile act as additional diffracting edges that scatter sound waves advancing over the profile leaving less sound energy to be diffracted into the shadow zone.

The barrier with the rounded cap had little effect in comparison to the plane barrier. It is possible that the absorptive material had degraded over time (the cap sections were over 7 years old) and therefore was not fully effective. Theory shows that a rounded edge is more effective in diffracting sound into the shadow zone than a classic ''knife-edge'' profile. If the absorptive material had been sufficiently degraded, there would be no improvement in screening performance.

The results of the study have also shown that wind effects can adversely affect the insertion loss of the options tested. This is small at low wind speeds but can become appreciable at higher speeds. This influence should be investigated further to fully quantify the effect. It may be possible to design profile shapes that not only improve performance in a static atmosphere but also utilize the wind to scatter sound away from the shadow zone and improve performance. Such improvements to a barrier have not been previously attempted and significant advances may result from a further study of these effects.

From a practical point of view, it is the performance in the far field that is generally of greater importance and therefore in any extension of the work the results of measurements made close to the barrier should be compared with results at greater distances [5]. In this way, the most appropriate measurement set-up for MLS-based measurements can be determined.

6. Conclusions

(i) A novel application of an MLS-based analysis approach has been developed experimentally and demonstrated to achieve a reliable and robust method for characterising the diffraction efficiency of noise barriers under realistic conditions.

(ii) The results of this study have established that the approach is sensitive enough to demonstrate differences between barrier profiles and the effects of wind vector.

(iii) Depending upon the barrier type or location, the current apparatus may require upgrading with a more powerful loudspeaker to improve the signal-to-noise ratio.

(iv) An absorptive T-shape and multiple-edge profiles were observed to offer the greatest improvement in screening performance over the plane screen.

(v) Further measurements are required to look at the effects on screening performance for angles of incidence other than normal incidence.

(vi) Wind effects can adversely affect the insertion loss of the barrier options tested. This is small at low wind speeds but can become appreciable at moderate and high speeds. It is suggested that further measurements be taken under a greater range of wind speeds to determine more precisely these differences.

(vii) The research reported here will enable in situ assessment and optimization of novel designs of noise barrier. Such a capability will be valuable to manufacturers in developing improved noise barriers and approving them for use, and in enabling Highways Authorities to obtain appraisals not previously available.

References

[1] European Committee for Standardisation, CEN/TS 1793-5. *Road Traffic Noise Reducing Devices–Test Method for Determining the Acoustic Performance—Part 5: Intrinsic Characteristics—In-situ Values of Sound Reflection and Airborne Sound Insulation*, CEN, Brussels, Belgium, 2003.

[2] D. Rife, J. Vanderkooy, Transfer function measurement with maximum length sequences, *Journal of the Audio Engineering Society* 37 (6) (1989) 419–433.

[3] G.R. Watts, D.H. Crombie, D.C. Hothersall, Acoustic performance of new designs of traffic noise barriers: full scale tests, *Journal of Sound and Vibration* 177 (3) (1994) 289–305.

[4] G.R. Watts, Acoustic performance of a multiple-edge noise barrier profile at motorway sites, *Applied Acoustics* 47 (1996) 47–66.
[5] S.N. Chandler-Wilde, Tyndall Medal lecture: the boundary element method in outdoor noise propagation, *Proceedings of the Institute of Acoustics* 19 (8) (1997) 27–50.
[6] A.J. Burton, G.F. Miller, The application of integral equation methods to the numerical solution of some exterior boundary value problems, *Proceedings of the Royal Society of London* A323 (1971) 201–210.
[7] European Committee for Standardisation, EN 1793-3. *Road Traffic Noise Reducing Devices–Test Method for Determining the Acoustic Performance—Part 3: Normalised Traffic Noise Spectrum*, CEN, Brussels, Belgium, 1997.